

Phase structure of QC_2D at high temperature and density

Seamus Cotter, Jon-Ivar Skullerud*

*Department of Mathematical Physics, National University of Ireland Maynooth,
Maynooth, County Kildare, Ireland*

E-mail: jonivar@thphys.nuim.ie

Pietro Giudice, Simon Hands

*Department of Physics, College of Science, Swansea University, Singleton Park, Swansea SA2
8PP, Wales, UK*

Seyong Kim

Department of Physics, Sejong University, Gunja-Dong, Gwangjin-Gu, Seoul 143-747, Korea

Dhagash Mehta

Department of Physics, Syracuse University, Syracuse, NY 13244, USA

We study two-color QCD with two flavors of Wilson fermion as a function of quark chemical potential μ and temperature T . We find evidence of a superfluid phase at intermediate μ and low T where the quark number density and diquark condensate are both very well described by a Fermi sphere of nearly-free quarks disrupted by a BCS condensate. This gives way to a region of deconfined quark matter at higher T and μ , with the deconfinement temperature decreasing only very slowly with increasing chemical potential. We find that heavy quarkonium bound states persist in the S-wave channels at all T and μ , with an energy reflecting the phase structure. P-wave states appear not to survive in the quarkyonic region.

*The 30th International Symposium on Lattice Field Theory
June 24 - 29, 2012
Cairns, Australia*

*Speaker.

1. Introduction

Our understanding of the phase structure of QCD at high baryon density and low temperature remains severely hampered by the sign problem. In the absence of first-principles methods which have been proven to circumvent this problem, we can study a related theory, QCD with colour group $SU(2)$ (QC_2D), which does not suffer from the sign problem. This may firstly allow us to confront model studies with lattice results, thereby constraining these models in their application to real QCD, and secondly reveal generic features of the phase structure of strongly interacting gauge theories, including the nature of deconfinement at high density.

Here we present an update of our ongoing investigation of the phase structure of QC_2D as a function of temperature and chemical potential [1, 2].

2. Simulation details

We study two-colour QCD with a conventional Wilson action for the gauge fields and two flavours of unimproved Wilson fermion. The fermion action is augmented by a gauge- and iso-singlet diquark source term which serves the dual purpose of lifting the low-lying eigenvalues of the Dirac operator and allowing a controlled study of diquark condensation. Further details about the action and the Hybrid Monte Carlo algorithm used can be found in [3]. We have performed simulations at $\beta = 1.9$, $\kappa = 0.168$, corresponding to a lattice spacing $a = 0.178\text{fm}$, determined from the string tension, and a pion mass $am_\pi = 0.645$ or $m_\pi \approx 710\text{MeV}$. The ratio of the ground state pseudoscalar to vector masses is $m_\pi/m_\rho = 0.80$ [4]. Our lattice volumes and the corresponding values for temperatures T , chemical potentials μ and diquark sources j are given in table 1. All results shown are extrapolated to $j = 0$ using a linear Ansatz except where otherwise stated.

N_s	N_τ	T (MeV)	μa	ja
16	24	47	0.3–0.9	0.04
12	24	47	0.25–1.1	0.02, 0.03, 0.04
12	16	70	0.3–0.9	0.04
16	12	94	0.2–0.9	0.02, 0.04
16	8	141	0.1–0.9	0.02, 0.04

Table 1: Lattice volumes and associated temperatures T , chemical potentials μ and diquark sources j .

3. Order parameters and phase structure

The left panel of fig. 1 shows the diquark condensate $\langle qq \rangle = \langle \psi^{2tr} C \gamma_5 \tau_2 \psi^1 - \bar{\psi}^1 C \gamma_5 \tau_2 \bar{\psi}^{2tr} \rangle$ as a function of chemical potential, for the $N_\tau = 24, 12$ and 8 lattices. In the case of a weakly-coupled BCS condensate at the Fermi surface, the diquark condensate, which is the number density of Cooper pairs, should be proportional to the area of the Fermi surface, ie $\langle qq \rangle \sim \mu^2$.

For the lowest temperature, $T = 47$ MeV ($N_\tau = 24$), we see that $\langle qq \rangle / \mu^2$ has a plateau in the region $0.35 \lesssim \mu a \lesssim 0.6$. The increase for $\mu a \gtrsim 0.6$ may be evidence of a transition to a new state of matter at high density, although the impact of lattice artefacts cannot be excluded. The lower limit

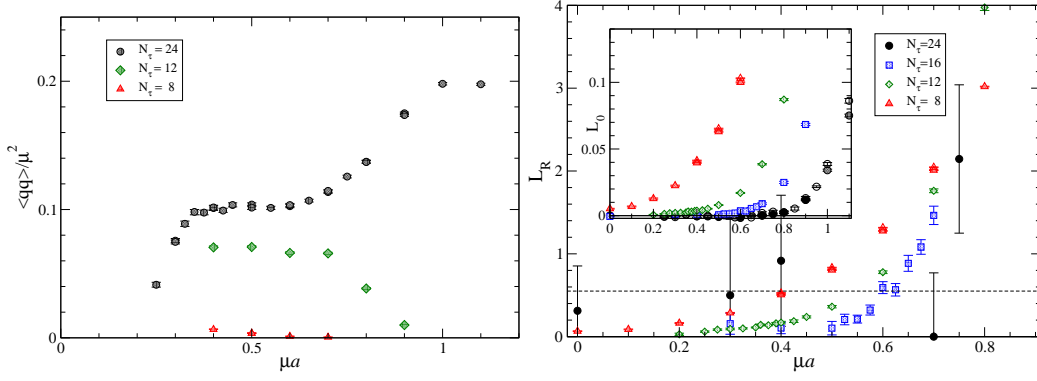


Figure 1: Left: The diquark condensate $\langle qq \rangle / \mu^2$ extrapolated to $j = 0$ for $N_\tau = 24, 12, 8$ ($T = 47, 94, 141$ MeV). Right: The renormalised Polyakov loop as a function of chemical potential, for all temperatures. The shaded symbols are for $ja = 0.04$; the open symbols are $ja = 0.02$. The filled black circles are the results for the $16^3 \times 24$ lattice. The dashed line indicates the inflection point of L at $\mu = 0$. The inset shows the unrenormalised Polyakov loop.

of the plateau roughly coincides with the onset chemical potential $\mu_o \approx m_\pi/2 \approx 0.33a^{-1}$, below which both the quark number density and diquark condensate are expected to be zero. We find no substantial volume dependence at any μ . Our results at $T = 70$ MeV (not shown here) are almost identical to those at $T = 47$ MeV. At $T = 94$ MeV ($N_\tau = 12$), $\langle qq \rangle$ is significantly suppressed, and drops dramatically for $\mu a \gtrsim 0.7$. At $T = 141$ MeV ($N_\tau = 8$) the diquark condensate is zero at all μ , confirming that the system is in the normal phase at this temperature.

In the right panel of fig. 1 we show the order parameter for deconfinement, the Polyakov loop L , for our four temperatures. It has been renormalised by requiring $L(Ta = \frac{1}{4}, \mu = 0) = 1$, see [1] for details. We see that for each temperature T , L increases rapidly from zero above a chemical potential $\mu_d(T)$ which we may identify with the chemical potential for deconfinement. In the absence of a more rigorous criterion, we have taken the point where L crosses the value it takes at $T_d(\mu = 0)$, $L_d = 0.6$ [1], to define $\mu_d(T)$. The results are shown in fig. 2, with error bars denoting the range $L_d = 0.5-0.7$. To more accurately locate the deconfinement line, we will need to perform a temperature scan for fixed μ -values. This is underway.

The estimates of critical chemical potentials for deconfinement and superfluidity can be translated into a tentative phase diagram, shown in fig. 2. In summary, from the order parameters we find signatures of three different regions (or phases): a normal (hadronic) phase with $\langle qq \rangle = 0$, $\langle L \rangle \approx 0$; a BCS (quarkyonic) region with $\langle qq \rangle \sim \mu^2$ at low T and intermediate to large μ ; and a deconfined, normal phase with $\langle qq \rangle = 0$, $\langle L \rangle \neq 0$ at large T and/or μ . After extrapolating our results to $j = 0$ we see no evidence of a BEC region described by χ Pt, with $\langle qq \rangle \sim \sqrt{1 - \mu_o^4/\mu^4}$ [5], in contrast with earlier work with staggered lattice fermions [6]. This may be related to the large value of m_π/m_ρ in this study. Simulations with lighter quarks may yield further insight into this.

In the right panel of fig. 2 we show the static quark potential computed from the Wilson loop at $N_\tau = 24$, for $\mu a = 0.3, 0.5, 0.7, 0.9$. We find that as we enter the superfluid region, the string tension is slightly reduced, but that this is reversed as μ is increased further, leading to a strongly enhanced string tension at $\mu a = 0.9$, which according to our analysis of the Polyakov loops should be in the deconfined region. This agrees with the pattern that was already observed in [3]. We also

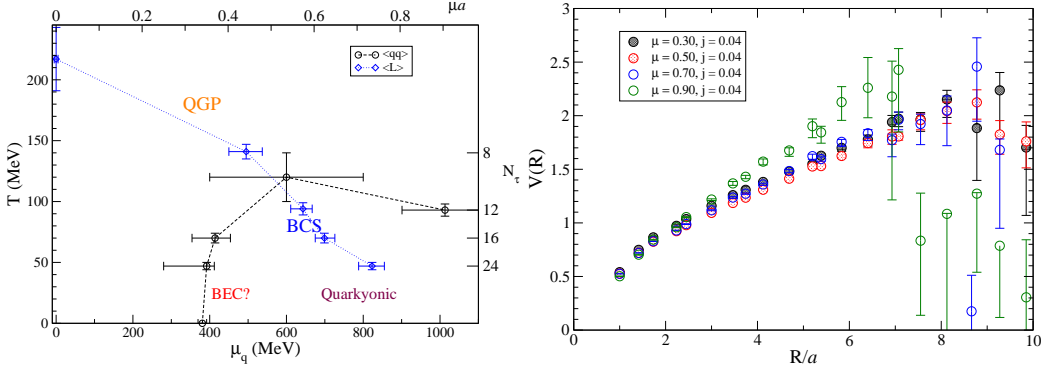


Figure 2: Left: A tentative phase diagram, including the location of the deconfinement transition in the (μ, T) plane, determined from the renormalised Polyakov loop, and the transition to the diquark condensed $\langle qq \rangle \neq 0$ phase. Right: The static quark potential computed from the Wilson loop, for the $12^3 \times 24$ lattice and different values of μ .

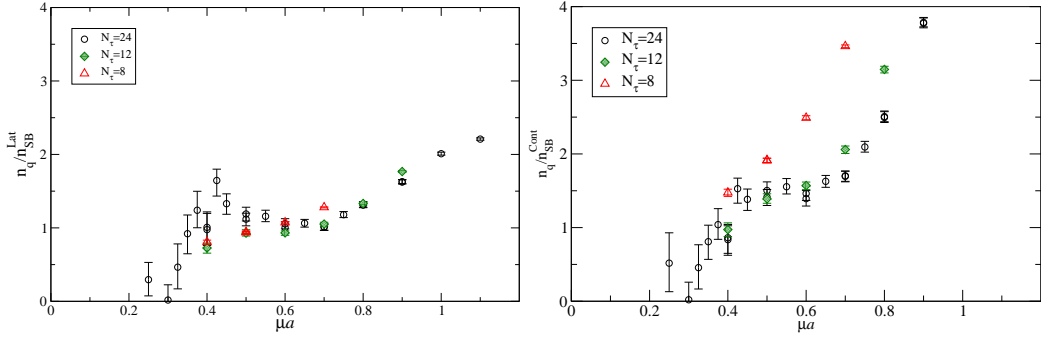


Figure 3: The quark number density divided by the density for a noninteracting gas of lattice quarks (left) and continuum quarks (right).

find no significance j -dependence in our results. At present we do not have a good understanding of why the static quark potential should become antiscreened at large μ . Computing the static quark potential using Polyakov loop correlators rather than Wilson loops may yield further insight into this issue.

4. Equation of state

We now turn to the bulk thermodynamics of the system, and in particular the quark number n_q and the energy density ε . Fig. 3 shows the quark number density n_q for $N_\tau = 24, 12$ and 8 , extrapolated to zero diquark source, and normalised by the noninteracting value for lattice fermions on the left and for continuum fermions on the right. The difference between the two gives an indication of the lattice artefacts. We see that the density rises from zero at $\mu \approx \mu_0 = 0.32a^{-1}$, and for the two lower temperatures is roughly constant and approximately equal to the noninteracting fermion density in the region $0.4 \lesssim \mu a \lesssim 0.7$. The peak at $\mu a \simeq 0.4$ in the $N_\tau = 24$ data in the upper panel is an artefact of the normalisation with n_{SB} for a finite lattice volume: the raw numbers for the $12^3 \times 24$ and $16^3 \times 24$ lattices are identical within errors, but n_{SB} differs by about 50% around $\mu a = 0.4$.

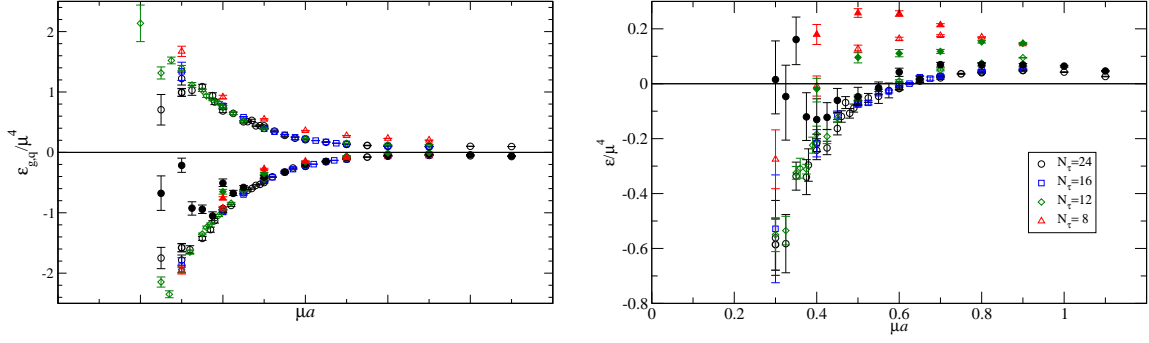


Figure 4: The quark and gluon contributions to the energy density (left) and total energy density (right), divided by μ^4 , for $ja = 0.04$ (open symbols) and $j = 0$ (filled symbols).

The density for $N_\tau = 8$ does not show any plateau as a function of μ ; instead, n_q/n_{SB} shows a roughly linear increase in the region $0.4 \leq \mu a \leq 0.7$. This is suggestive of the system being in a different phase at this temperature. We also note that n_q/n_{SB} for $N_\tau = 12$ rises above the corresponding $N_\tau = 24$ data for $\mu a \gtrsim 0.7$, where, according to the results of Sec. 3, the hotter system is entering the deconfined, normal phase.

These results lend further support to our previous conjecture that in the intermediate-density, low-temperature region the system is in a ‘‘quarkyonic’’ phase: a confined phase (all excitations are colourless) that can be described by quark degrees of freedom.

The renormalised energy density can be derived by going to an anisotropic lattice formulation with bare anisotropies $\gamma_g = \sqrt{\beta_t/\beta_s}$, $\gamma_q = \kappa_t/\kappa_s$ and physical anisotropy $\xi = a_s/a_\tau$. In the isotropic limit $\gamma_q = \gamma_g = \xi = 1$ the energy density is then given by $\varepsilon = \varepsilon_g + \varepsilon_q$ with

$$\varepsilon_g = \frac{3}{2a^4} \left[\langle \text{Re Tr } U_{ij} \rangle \left(\frac{\partial \beta}{\partial \xi} - \beta \frac{\partial \gamma_g}{\partial \xi} \right) + \langle \text{Re Tr } U_{i0} \rangle \left(\frac{\partial \beta}{\partial \xi} + \beta \frac{\partial \gamma_g}{\partial \xi} \right) \right], \quad (4.1)$$

$$\varepsilon_q = \frac{1}{a^4} \left[\kappa^{-1} \frac{\partial \kappa}{\partial \xi} (16 + \langle \bar{\psi} \psi \rangle) - \kappa \frac{\partial \gamma_q}{\partial \xi} \langle \bar{\psi} D_0 \psi \rangle \right]. \quad (4.2)$$

We have determined the Karsch coefficients $\partial c_i / \partial \xi$ with $c_i = \gamma_g, \gamma_q, \beta, \kappa$ by performing simulations with $\gamma_q, \gamma_g \neq 1$. Our estimates for these coefficients are [1]

$$\frac{\partial \gamma_g}{\partial \xi} = 0.90_{-14}^{+4}, \quad \frac{\partial \gamma_q}{\partial \xi} = 0.13_{-5}^{+40}, \quad \frac{\partial \beta}{\partial \xi} = 0.59_{-1.37}^{+0.24}, \quad \frac{\partial \kappa}{\partial \xi} = -0.052_{-15}^{+69}. \quad (4.3)$$

Our results for the energy density are shown in fig. 4. We see that the quark contribution is negative for all values of μ and T , but this is balanced by the positive gluon contribution, giving a positive or zero total energy. The energy density is very sensitive to the values of the Karsch coefficients [1]; for example, if $\partial \gamma_q / \partial \xi$ is changed from the surprisingly low value of 0.13 to a more ‘natural’ value of 0.8, we find that $\varepsilon_q > 0$ for $\mu a \gtrsim 0.6$.

5. Heavy quarkonium

We have investigated the heavy quarkonium spectrum by computing non-relativistic QC_2D correlators on our $N_\tau = 24, 16$ and 12 lattices. We use an $\mathcal{O}(v^4)$ lattice NRQCD lagrangian [7]

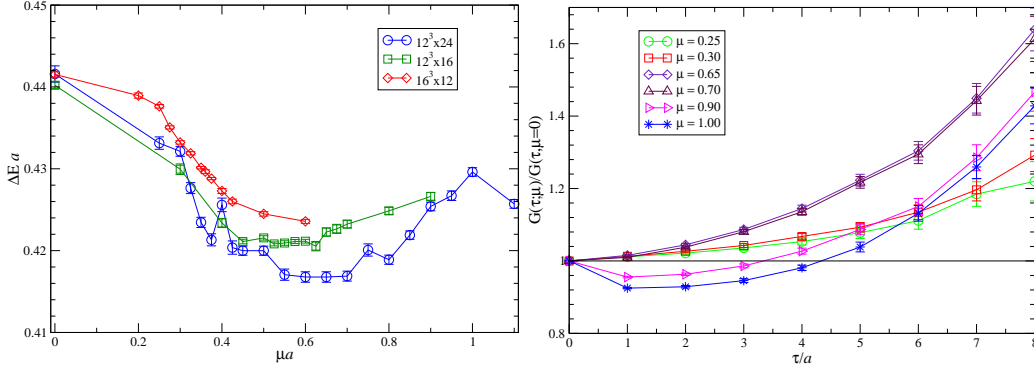


Figure 5: Left: Temperature dependence of the 1S_0 state energy vs. μ for $Ma = 5.0$ with $j = 0.04$. Right: The ratio $\sum_{\mathbf{x}} G(\mathbf{x}, \tau; \mu) / \sum_{\mathbf{x}} G(\mathbf{x}, \tau; 0)$ for 1P_0 correlators on $12^3 \times 24$ with $Ma = 5.0$. Due to the noisiness of the P-wave data, only a limited τ range is shown.

to compute the heavy quark Green function; see [2] for further details. We find that the S-wave correlators can be fitted with an exponential decay $\propto e^{-\Delta E_n \tau}$ even once $\mu \neq 0$; moreover the fits are quite stable over large ranges of τ , indicating that S-wave bound states persist throughout the region $47 \text{ MeV} \lesssim T \lesssim 90 \text{ MeV}$.

Fig. 5 shows the T - and μ -dependences of the 1S_0 state energy ΔE . We see that as μ is varied, initially the 1S_0 state energy decreases from that at $\mu = 0$, but once μ reaches the region $\mu_1 (\simeq 0.5) \leq \mu a \leq \mu_2 (\simeq 0.85)$, the 1S_0 state energy stays roughly constant. For $\mu > \mu_2$, the 1S_0 state energy starts increasing again. In contrast to the observables studied in Secs 3 and 4, we find no clear, systematic dependence on the diquark source term for $\mu a \lesssim 0.5$. For $\mu a \gtrsim 0.5$ on the other hand, $\Delta E(ja = 0.02) < \Delta E(ja = 0.04)$. This suggests that the energy, extrapolated to $j = 0$, may continue to decrease up to $\mu a \approx 0.7$ before increasing.

As the temperature increases from 47 MeV ($N_\tau = 24$) to 70 MeV ($N_\tau = 16$) we find that the point where the energy of the 1S_0 state starts increasing goes from $\mu a \approx 0.7$ to 0.55. This is consistent with the estimate of the deconfinement transition in Sec. 3. For $N_\tau = 12$ we do not yet have any data in the μ -region which might confirm this. It is interesting to note that ΔE increases with increasing T , in accordance with what has been observed in hot QCD with $\mu = 0$ [8].

In contrast to the S-waves, it is difficult to find stable exponential fits to the P-wave correlators with the current Monte-Carlo data before statistical noise sets in, except for the case $\mu a \leq 0.25$. In the right panel of fig. 5 we instead show the ratios of the 1P_0 correlators at different values $\mu \neq 0$ to the correlator at $\mu = 0$. Note that any effect we observe is entirely due to the dense medium.

The S-wave correlator ratios show an increase with τ which corresponds to the negative 1S_0 energy difference $\Delta E(\mu) - \Delta E(\mu = 0)$ that was previously observed. In the quarkyonic region, the P-wave ratios behave similarly to the S-wave, but in the deconfined region ($\mu \geq \mu_2$), the P-wave ratios are non-monotonic, initially decreasing with τ before turning to rise above unity for $\tau/a \sim 4$. On the other hand, the P-wave correlator ratios on the $12^3 \times 16$ and $16^3 \times 12$ lattice show monotonic behavior similar to those of the S-waves, suggesting a subtle interplay of density and temperature effects on the P-wave states.

6. Summary and outlook

From lattice simulations of dense QC_2D at a range of temperatures, we have identified three distinct regions of the phase diagram: a hadron gas at low μ and T , a quarkyonic region at intermediate μ and low to intermediate T , and a deconfined quark–gluon plasma at high T and/or μ . Taking the limit of zero diquark source has served to make our identification of the quarkyonic region more robust. Investigations into the exact nature and location of the deconfinement and the superfluid to normal transitions are underway, as are simulations at smaller lattice spacings and with smaller quark masses.

Acknowledgments

This work is carried out as part of the UKQCD collaboration and the DiRAC Facility jointly funded by STFC, the Large Facilities Capital Fund of BIS and Swansea University. We thank the DEISA Consortium (www.deisa.eu), funded through the EU FP7 project RI-222919, for support within the DEISA Extreme Computing Initiative, and the USQCD for use of computing resources at Fermilab. JIS and SC acknowledge the support of Science Foundation Ireland grants 08-RFP-PHY1462, 11-RFP.1-PHY3193 and 11-RFP.1-PHY3193-STTF-1. SK is grateful to STFC for a Visiting Researcher Grant and is supported by the National Research Foundation of Korea grant funded by the Korea government (MEST) No. 2011-0026688. DM acknowledges support from the U.S. Department of Energy under contract no. DE-FG02-85ER40237. JIS acknowledges the support and hospitality of the Institute for Nuclear Theory at the University of Washington, where part of this work was carried out.

References

- [1] S. Cotter, P. Giudice, S. Hands and J.-I. Skullerud, *Towards the phase diagram of dense two-color matter*, 1210.4496.
- [2] S. Hands, S. Kim and J.-I. Skullerud, *Non-relativistic spectrum of two-color QCD at non-zero baryon density*, *Phys.Lett.* **B711** (2012) 199–204 [1202.4353].
- [3] S. Hands, S. Kim and J.-I. Skullerud, *Deconfinement in dense 2-color QCD*, *Eur. Phys. J.* **C48** (2006) 193 [hep-lat/0604004].
- [4] S. Hands, S. Kim and J.-I. Skullerud, *A quarkyonic phase in dense two color matter?*, *Phys. Rev.* **D81** (2010) 091502 [1001.1682].
- [5] J. Kogut, M. Stephanov, D. Toublan, J. Verbaarschot and A. Zhitnitsky, *QCD-like theories at finite baryon density*, *Nucl. Phys.* **B582** (2000) 477 [hep-ph/0001171].
- [6] S. Hands, I. Montvay, S. Morrison, M. Oevers, L. Scorzato and J. Skullerud, *Numerical study of dense adjoint matter in two color QCD*, *Eur. Phys. J.* **C17** (2000) 285–302 [hep-lat/0006018].
- [7] G. T. Bodwin, E. Braaten and G. P. Lepage, *Rigorous QCD analysis of inclusive annihilation and production of heavy quarkonium*, *Phys.Rev.* **D51** (1995) 1125–1171 [hep-ph/9407339].
- [8] G. Aarts, C. Allton, S. Kim, M. Lombardo, M. Oktay *et. al.*, *What happens to the Υ and η_b in the quark-gluon plasma? Bottomonium spectral functions from lattice QCD*, *JHEP* **1111** (2011) 103 [1109.4496].